Wideband Differential-Mode Bandpass Filters With Stopband and Common-Mode Suppression

Khaled Aliqab, *Student Member, IEEE*, and Jiasheng Hong, *Fellow IEEE*

***Abstract*—This paper presents wideband differential-mode bandpass filters (BPFs) designed on a microstrip line for ultra-wideband (UWB) applications. The proposed design is based on an optimized branch-line structure with extended transmission lines (TLs). An enhanced performance can be obtained using a very simple design approach. The introduced TLs can be used for improving the differential-mode stopband response by introducing multiple transmission zeros (TZs) at the lower and upper stopband. The common-mode rejection level can also achieve around 40 dB within the band of interest. The proposed filters are fabricated for experimental verification. The predicted and measured results show a very good agreement.**

***Index Terms*—Balanced bandpass filters (BPF), common-mode suppression, ultra-wideband (UWB).**

I. Introduction

BANDPASS filters (BPFs) with low cost, high performance and compact size are key components in any communication system. Since the use of the unlicensed ultra-wideband (UWB) systems has been authorized by the Federal Communication Commission (FCC), an increasing interest amongst both academic and industrial researchers is growing towards this technology.

Recently, balanced/differential-mode microwave filters have received much more interest from the microwave community due to the increasing demand for balanced circuits and systems. Balanced transceivers differentially operating are much more immune to noise, crosstalk and electromagnetic interference in comparison to their single-ended counterparts. In this aspect, numerous wideband BPFs have been reported following various approaches.

In [1], a differential-mode bandpass filter is presented with common-mode suppression. However, the proposed design is only applicable for narrow band applications. A structure based on branch-line with additional open-circuited stubs is shown in [2]. It demonstrates a wide differential-mode passband as well as a common-mode stopband but the circuit size is a little large. In [3], wideband differential BPFs are presented based on T-shaped structure. Yet, the common-mode suppression is limited. Another class of wideband differential-mode BPF for UWB applications is proposed in [4], but with poor frequency selectivity and common-mode suppression. Based on the transversal signal-interference concept, a differential UWB BPF is presented in [5], which results in poor differential and common-mode responses due to the sensitivity of the design proposed.

Manuscript received xxxx xx, xxxx; revised xxx xx, xxxx; accepted xxx xx, xxxx. This work was supported by Al-Jouf University, Sakaka, Saudi Arabia. (*Corresponding author: Khaled Aliqab*)

K. Aliqab and J. Hong are with the School of Engineering & Physical Sciences, Heriot-Watt University, Edinburgh, EH14 4AS, UK. (e-mail: kma20@hw.ac.uk; j.hong@hw.ac.uk)

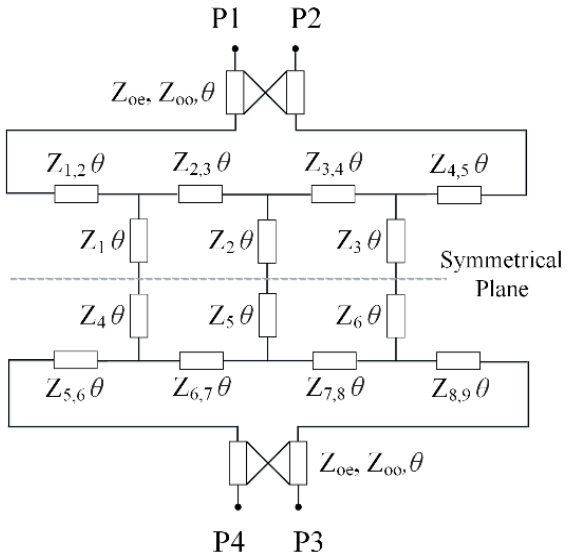

Fig.1. Topology of the proposed wideband BPFs.

In this letter, two wideband differential-mode BPFs centred at 6.85 GHz with high selectivity, compact size and intrinsic common-mode suppression are proposed and constructed on a microstrip line. They are constituted in an optimized branch-line configuration with extended TLs at the I/O ports. Two prototypes are designed and fabricated where the simulated and measured results are in a good agreement.

II. Analysis & Design

Fig. 1 illustrates the proposed design schematic in which Z_i and $Z_{i,j}$ represent the branch-line stubs and the connecting lines respectively. In order to improve the selectivity and enhance the group delay of the filter with minimal resonators used, extended TLs at the I/O ports are introduced. As it can be seen from Fig. 1 that the proposed design is ideally symmetric with respect to the dotted-line (central plane). Therefore, this plane can be considered as a perfect electric or magnetic wall depending on the type of excitation applied at the paired input ports (P1 and P4), or output ports (P2 and P3). Although the proposed design consists of only n stubs, it is capable of having an insertion function of $2n$-1 degree in frequency under differential-mode excitation as a result of having four nonredundant unit elements and one short-circuited stub in a canonical form. Two TZs at dc and at $2f_0$ are generated as expected. On both sides of the primary passband, two extra TZs can be observed using I/O cross-coupling, which can be split and allocated at different

frequencies leading to a better stopband and selectivity. Computer-aided design (CAD) programs or some commercially available design tools, AWR Microwave office, for instance can be utilized for circuit parameters calculations. Table I shows the set of circuit parameters optimized for this wideband differential-mode BPFs with extended TLs at the I/O ports. The introduced extended TLs at the feeding ports can be configured in two different ways. They can be coupled together (P1 with P2 and P4 with P3) in which even and odd mode impedances Z_e and Z_o are used to represent this relationship as shown in case (1). On the other hand, these TLs can have no or very weak coupling as shown in case (2).

TABLE I
CIRCUIT PARAMETERS FOR THE PROPOSED WIDEBAND BPF (θ=90° AT f_0)

Stub line	Connecting line	Coupled line
Z_1=Z_3=Z_4=Z_6= 36.1Ω	$Z_{1,2}$= $Z_{4,5}$= $Z_{5,6}$= $Z_{8,9}$= 106.1Ω	Case (1): Z_{oe}= 97.5Ω, Z_{oo}= 83.9Ω
Z_2=Z_5= 24Ω	$Z_{2,3}$= $Z_{3,4}$= $Z_{6,7}$= $Z_{7,8}$= 71.9Ω	Case (2): Z_{oe}= Z_{oo}= 90.2Ω

The two-port transmission characteristics of the differential and common-modes for the balanced filter can be derived from the four-port scattering parameters using the following equations [6]:

$$S_{11,\,DD} = (S_{11} - S_{41} - S_{14} + S_{44})/2 \quad (1)$$
$$S_{21,\,DD} = (S_{21} - S_{31} - S_{24} + S_{34})/2 \quad (2)$$
$$S_{11,\,CC} = (S_{11} + S_{41} + S_{14} + S_{44})/2 \quad (3)$$
$$S_{21,\,CC} = (S_{21} + S_{31} + S_{24} + S_{34})/2 \quad (4)$$

Fig. 2 illustrates the circuit model frequency response. The proposed design demonstrates a wideband performance with 58% fractional bandwidth (FBW) centred at 6.85 GHz. As it is shown in Fig. 2, five transmission-poles are generated (n=3) within the wideband differential-mode passband as expected. The bandwidth of this design can also be controlled by carefully optimizing the even and odd mode impedances.

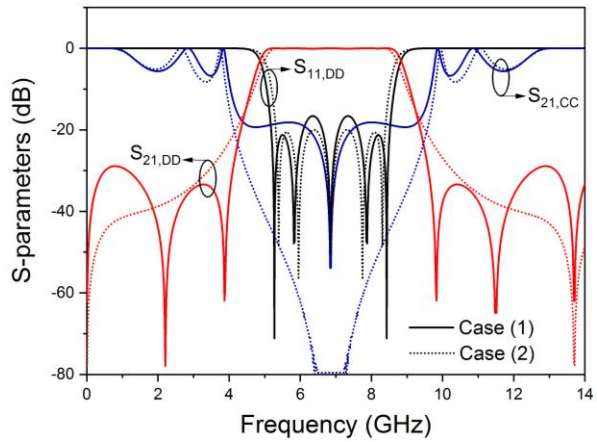

Fig.2. Circuit model frequency response.

Fig. 2 represents the frequency response for both cases in Table I. In case (1), where a strong coupling between the I/O extended TLs is introduced, resulting in multiple TZs at the lower and upper sides of the passband so that both passband selectivity and stopband performance are enhanced. The common-mode rejection ($S_{21,cc}$) also maintains at a great level approaching 20 dB throughout the entire passband.

On the other hand, in case (2) where no coupling exists between the I/O extended TLs, an outstanding common-mode rejection level better than 40 dB is obtained.

The final optimized layouts of the wideband differential-mode BPFs, designed using full-wave EM simulator (Sonnet), are shown in Fig. 3. Final dimensions for case (1) are as follows: L1=6.9, L2=6.5, L3=1.1, L4=13.8, W1=0.5, W2=0.3, W3=0.7, W4=3.4 and W5=2.6. Final dimensions for case (2) are as follows: L1=7.2, L2=13.8, W1=0.5, W2=0.3, W3=0.7, W4=3.4 and W5=2.6 (all in millimetres). The proposed designs were manufactured using the conventional PCB fabrication techniques for microstrip designs. Rogers RO3003 substrate with a dielectric constant of 3.0, a loss tangent of 0.0025 and a thickness of 0.5 mm was utilized.

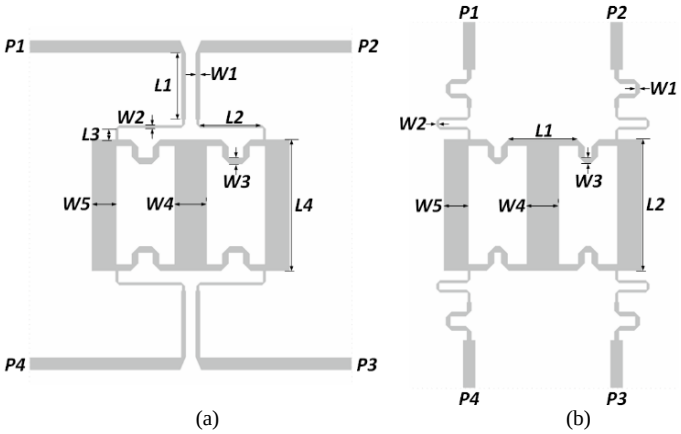

Fig.3. (a) Case (1). (b) Case (2).

III. MEASUREMENT & DISCUSSION

Based on the above discussion, two wideband differential-mode BPFs centred at 6.85 GHz with a FBW of 58% were designed, simulated and fabricated. They were manufactured in-house and an N5225A PNA Microwave Network Analyser was used to obtain the final measurement results.

Fig. 4 shows the simulated and measured frequency responses plotted together on the same graph for comparison for both filters illustrating the differential and common-mode responses. Across the desired wide passband, for case (1): the measured differential-mode return loss $|S_{11,DD}|$ is better than 11.6 dB whereas the differential-mode insertion loss $|S_{21,DD}|$ is not more than 0.8 dB as demonstrated in Fig. 4(a). On the other hand, the measured common-mode insertion loss $|S_{21,CC}|$ is better than 13 dB within the entire band of interest. For case (2): the measured differential-mode return loss $|S_{11,DD}|$ and insertion loss $|S_{21,DD}|$ are better than 10.5 dB and 0.7 dB respectively as demonstrated in Fig. 4(b). The measured common-mode insertion loss $|S_{21,CC}|$ for this case is better than 38 dB throughout the entire band of interest.

As it is clearly shown, that both the simulated and measured results highly agree with each other. The relative discrepancies between the simulated and the measured frequency responses are attributed to fabrication tolerances. That, as a result, introduces losses and affects the design symmetry, which as a

consequence, influences both the differential and common-mode responses. In addition, perfect symmetry is extremely difficult to obtain in practice.

This proposed I/O extended TLs relationship can be used for optimizing the stopband rejection by introducing multiple TZs or can be used for improving the common-mode rejection level throughout the passband. When coupling is introduced between the TLs as in case (1), the even and odd-mode impedances can be used for controlling the lower and upper stopbands by introducing multiple TZs within. Alternatively, when no coupling between the TLs exists, a remarkable common-mode rejection extending throughout the entire passband is achieved.

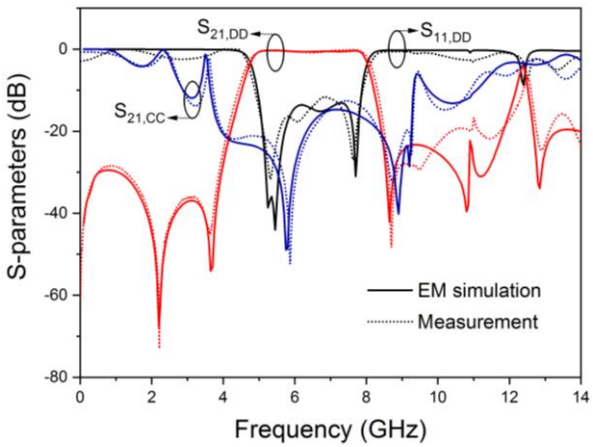

Fig.4. EM simulation and measurement frequency responses. (a) Case (1). (b) Case (2).

Fig. 5 illustrates the simulated and measured group delays of the proposed differential-mode BPFs. The in-band group delays of the implemented designs are all flat throughout the whole passband.

The proposed designs are compared with other related wideband BPFs designs from the literature as shown in Table II. It includes the centre operating frequency f_0, the differential-mode fractional bandwidth DM-FBW, the effective circuit size in terms of the guided wavelength λ_g^2, and finally the common-mode rejection level $|S_{21,\,CC}|$. The wideband differential-mode BPF presented in case (2) in this paper illustrates an outstanding common-mode rejection level better than 38 dB extending throughout the entire passband. In addition, the size of the proposed filters are relatively compact in comparison to the other reported work. That, with the simplicity of the design indicates potential application in communication systems especially in Ultra-wideband designs.

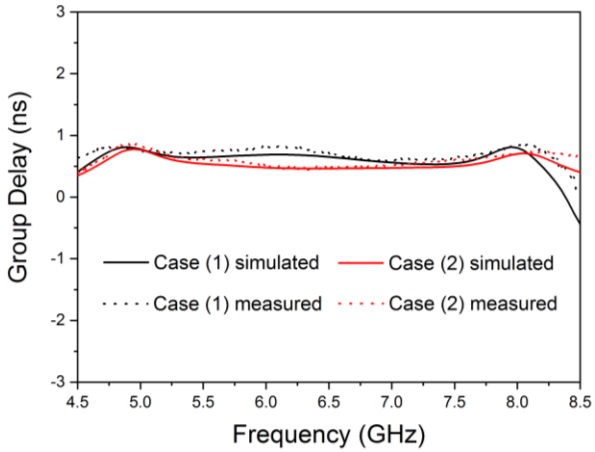

Fig.5. Simulated and measured group delays.

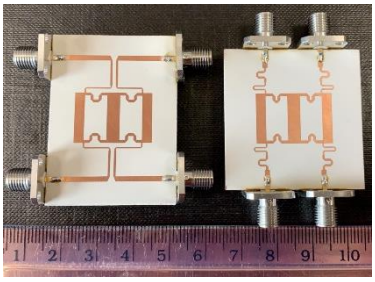

Fig.6. Photos of fabricated filters.

TABLE II
PERFORMANCE COMPARISON WITH OTHER WORKS

Ref.	f_0 (GHz)	DM-FBW (3-dB)	Size (λ_g^2)	In-band $\lvert S_{21,\,CC}\rvert$ (dB)
[3]	6.85	70%	1.1	-14.5
[7]	1.5	43%	0.13	-20
[8]	5.0	22%	0.4	-20
[9]	5.94	61%	0.45	-15.7
[10]	6.8	67.6%	1.38	-15
[11]	5.08	38%	1.27	-17
Case (1)	**6.85**	**58%**	**1.0**	**-13**
Case (2)	**6.85**	**58%**	**0.98**	**-38**

IV. CONCLUSIONS

Two wideband balanced BPFs with differential-mode stopband and intrinsic common-mode rejections are presented. Input and output (I/O) extended TLs are introduced to the branch-line structure to be able to control both the differential and common-mode responses. The proposed approach demonstrates the flexibility and capability of improving the stopband rejection for the differential-mode and/or the rejection level for the common-mode responses.

REFERENCES

[1] C.-H. Wu, C.-H. Wang, and C. H. Chen, "Balanced coupled-resonator bandpass filters using multisection resonators for common-mode suppression and stopband extension," *IEEE Trans. Microw. Theory Tech.*, vol. 55, no. 8, pp. 1756–1763, Aug. 2007.

[2] T. B. Lim and L. Zhu, "A differential-mode wideband bandpass filter on microstrip line for UWB application," *IEEE Microw. Wireless Compon. Lett*., vol. 19, no. 10, pp. 632–634, Oct. 2009.

[3] W. J. Feng and W. Q. Che, "Novel wideband differential bandpass filters based on T-shaped structure," *IEEE Trans. Microw. Theory Tech.*, vol. 60, no. 6, pp. 1560–1568, Jun. 2012.

[4] T. B. Lim and L. Zhu, "Differential-mode wideband bandpass filter with three transmission zeros under common-mode operation," in *Proc. Asia-Pacific Microw. Conf.*, pp. 159–162, Dec. 2009.

[5] H. T. Zhu, W. J. Feng, W. Q. Che, and Q. Xue, "Ultra-wideband differential bandpass filter based on transversal signal-interference concept," *Electron. Lett*., vol. 47, no. 18, pp. 1033–1035, Sep. 2011.

[6] D. E. Bockelman and W. R. Eisenstadt, "Combined differential and common-mode scattering parameters: Theory and simulation," *IEEE Trans. Microw. Theory Techn*., vol. 43, no. 7, pp. 1530–1539, Jul. 1995.

[7] M. Sans et al., "Optimized wideband differential-mode bandpass filters with broad stopband and common-mode suppression based on multisection stepped impedance resonators and interdigital capacitors," in *IEEE MTT-S Int. Microw. Symp. Dig*., Seville, Spain, pp. 10–12, May 2017.

[8] X. Gao, W. Feng, and W. Che, "High-selectivity wideband balanced filters using coupled lines with open/shorted stubs," *IEEE Microw. Wireless Compon. Lett*., vol. 27, no. 3, pp. 260–262, Mar. 2017.

[9] Q. Chu and L. Qiu, "Wideband balanced bandpass filter using slot resonators and back-to-back structure," *IEEE International Wirelesss Symposium*., pp. 1–4, Mar. 2015.

[10] W. Feng, W. Che, and Q. Xue, "Novel wideband balanced bandpass filter based on multi-mode resonator," *in Proc. 42nd Eur. Microw. Conf.*, pp. 392–395, Oct. 2012.

[11] X. Gao, W. Che, and W. Feng, "High selectivity wideband balanced filter based on modified coupled lines structures," in *10th Glob. Symp. on Millimeter-Waves*, pp. 47–49, May 2017.